FULL PAPER

Reductively Dissociable siRNA-Polymer Hybrid Nanogels for Efficient Targeted Gene Silencing

Cheol Am Hong, Jee Seon Kim, Soo Hyeon Lee, Won Ho Kong, Tae Gwan Park, Hyejung Mok, and Yoon Sung Nam**

A highly efficient approach for target-specific gene silencing based on a reductively dissociable nanogel incorporating small interfering RNA (siRNA) crosslinked with linear polyethylenimine (LPEI) via disulfide bonds is presented. Thiol-terminated siRNA at both 3′-ends is electrostatically complexed with thiol-grafted LPEI. The prepared siRNA/LPEI complex contains inter- and intramolecular linkages, generating a mutually crosslinked siRNA/LPEI nanogel (MCN) that exhibits excellent structural stability against the addition of heparin but is readily disintegrated to biologically active, monomeric siRNA upon exposure to reductive conditions. Accordingly, the highly condensed, stable MCN shows greatly enhanced cellular uptake and gene silencing efficiency compared to the siRNA/LPEI complexes without crosslinks or with only LPEI-mediated crosslinks.

1. Introduction

Recently, siRNA has received increasing attention for therapeutic applications due to its target-specific gene silencing via RNA interference (RNAi).[1,3] It is urgently needed to develop a safe, stable, efficient delivery system for siRNA therapeutics because intracellular processing is essential for gene suppression.[4,5] It has been well investigated that plasmid DNA can be effectively condensed with cationic polyelectrolytes via electrostatic complexation, producing stable nanoscale colloidal complexes, called polyplexes, in aqueous solution.[6,8] Unlike plasmid DNA, siRNA has a stiff structure with relatively low spatial charge density, which makes it difficult to form stable and compact nanocomplexes.[9,10] To increase the structural stability of nanoscale siRNA complexes, the use of an excess amount of cationic carriers has been attempted; however, it could increase nonspecific cytotoxicity.[11–13]

A variety of cationic polyelectrolytes have been studied to effectively encapsulate siRNA within nanosized complexes for efficient intracellular transport and gene silencing.[14–16] The charge density of siRNA and cationic carriers has been shown to determine the size and structural stability of siRNA polyplexes.[17,19] One promising way to stabilize siRNA polyplexes is to use cleavable, high molecular weight polyelectrolytes comprising cationic oligomers connected via biodegradable linkages, such as disulfide, hydrazone, ketal, and ester bonds.[20,23] The multimerization of cationic oligomers can increase the spatial charge density of the cationic carrier and allow the formation of stable siRNA complexes. The cationic polyelectrolytes are readily dissociated to oligomeric fragments in the cell, which can efficiently alleviate the cytotoxicity of siRNA delivery carriers.[24] Our recent study also suggests that the multimerization of siRNA via flexible linkers containing disulfide bonds can increase the gene silencing effect due to the increased charge density and chain flexibility of siRNA.[25] In particular, the synthesized multimeric siRNA can be effectively condensed into stable nanoscale complexes with oligomeric cationic electrolytes, such as linear polyethylenimine (LPEI), which has a molecular weight of 25 kDa, enhancing intracellular uptake and gene silencing without significant cytotoxicity. Monomeric siRNA was shown to form large aggregates that exhibit low transfection efficiency.

This study introduces a novel approach based on highly stable, compact hydrogel nanoparticles, called nanogels, incorporating siRNA that are generated via reductively cleavable crosslinking of siRNA with linear polyethylenimine (LPEI). Thiol-terminated siRNA at both 3′-ends were crosslinked with thiol-grafted LPEI via disulfide bonds. We hypothesized that the inter- and intramolecular bridging between siRNA and LPEI can effectively stabilize the polyplex structure, while the nanogel could be readily dissociated in the cytoplasm if reductively cleavable linkages are used as crosslinks. The siRNA nanogel was expected to facilitate the intracellular translocation and gene silencing effects of siRNA, which are often limited

C. A. Hong, J. S. Kim, Dr. S. H. Lee, Dr. W. H. Kong, Prof. T. G. Park, Prof. Y. S. Nam
Department of Biological Sciences
Korea Advanced Institute of Science and Technology
291 Daehak-ro, Yuseung-gu, Daejeon 305-701, Republic of Korea
E-mail: yoonsung@kaist.ac.kr
Prof. H. Mok
Department of Bioscience and Biotechnology
Konkuk University
Seoul 143-701, Republic of Korea
E-mail: hjmok@konkuk.ac.kr
Prof. Y. S. Nam
Department of Materials Science and Engineering
KAIST Institute for NanoCentury (KINC) and BioCentury (KIB)
Korea Advanced Institute of Science and Technology
291 Daehak-ro, Yuseung-gu, Daejeon 305-701, Republic of Korea

DOI: 10.1002/adfm.201200780

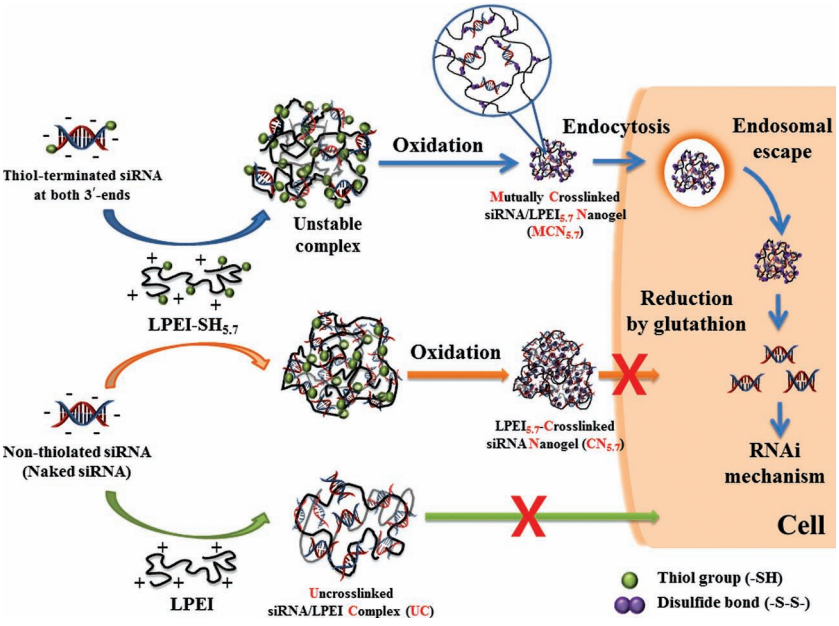

Figure 1. Schematic illustration for the preparation and intracellular processes of mutually crosslinked siRNA/$LPEI_{5.7}$ nanogels ($MCN_{5.7}$), $LPEI_{5.7}$-crosslinked siRNA nanogels ($CN_{5.7}$) and uncrosslinked siRNA/LPEI complexes (UC), respectively.

by the structural instability of polyplex.[26,27] Thiol-grafted LPEIs with different grafting densities of thiol groups were synthesized to control the crosslinking density of nanogels. The size distribution, zeta potential, morphology, structural stability, cellular uptake, and gene silencing efficiency of the prepared nanogels were determined and compared with those of nanoscale complexes prepared using naked siRNA with unmodified and thiol-grafted LPEI.

2. Results and Discussion

The preparation procedures of MCN are schematically illustrated in **Figure 1**. The electrostatic complexation between thiol-terminated siRNA and thiol-grafted LPEI is followed by the formation of stable nanogels chemically crosslinked via disulfide bonds between siRNA and LPEI. Thiol-terminated siRNA was prepared by hybridizing sense and antisense green fluorescence protein (GFP)-targeted siRNA primers, both of which were chemically modified with a thiol group at the 3′-end. To synthesize thiol-grafted LPEI, the secondary amines of LPEI with a molecular weight of 2.5 kDa were reacted with 2-methylthiirane via a ring-opening reaction.[20] The molar ratios of 2-methylthiirane to LPEI used in the feed were 1, 3, 5, and 9. The prepared thiol-grafted LPEI was denoted LPEI-SH_X, where X is the average number of thiol groups grafted to each LPEI backbone. The ratio of ethylene of LPEI to methyl of 2-methylthiirane of LPEI-SH_X was determined by ^{1}H NMR; the calculated X values were 1.2, 1.8, 5.7, and 7.3 (**Figure 2**).

To determine the kinetics of formation of disulfide bonds, the number of free thiol groups in various siRNA/LPEI-SH_X polyplexes, denoted MCN_X, at an N/P ratio of 60 was measured as a function of reaction time using Ellman's assay. Interestingly, more than 70% of the total number of linkages was generated in 1 h in all of MCN_X except $MCN_{1.2}$: only 45.8 ± 5.9%, 31.7 ± 1.9%, and 30.0 ± 5.6% of the initial thiol groups remained in $MCN_{1.8}$, $MCN_{5.7}$, and $MCN_{7.3}$, respectively, while a majority of free thiols (89.9 ± 3.3%) still remained in $MCN_{1.2}$ (**Figure 3**a). Following the electrostatic complexation, it seems likely that highly thiol-grafted LPEI-SH_X was more efficiently crosslinked presumably due to the high concentration and close proximity of thiol groups within individual polyplexes. The rapidly decreased rate of bond formation post 1 h reaction indicates that the chain mobility of siRNA and LPEI could decrease as the generated disulfide bonds could impose steric restriction for the residual free thiol groups. After 24 h, the numbers of free thiol groups in $MCN_{1.2}$, $MCN_{1.8}$, $MCN_{5.7}$, and $MCN_{7.3}$ were 75.0 ± 3.7%, 23.8 ± 3.0%, 8.3 ± 2.9%, and 7.6 ± 1.6%, respectively. This result indicates that a high level of thiol grafting to LPEI is required for the successful formation of a highly inter- and intra-connected nanogel comprising siRNA and LPEI.

We next determined whether the crosslinking density of MCN_X affects the size, surface charge, and structural stability of nanogels, which are critically important parameters determining the efficiency of intracellular delivery of nanogels. Uncrosslinked siRNA/LPEI polyplex, denoted UC, was also prepared as a control using naked siRNA and unmodified LPEI. The hydrodynamic size and zeta potential of various MCN_X and UC were determined, as shown in Figure 3b,c, respectively. UC formed micrometer-sized particles as commonly observed for siRNA polyplexes.[28] Interesting, only approximately one thiol group per LPEI chain induced the significant decreases in size compared to unmodified LPEI. At an N/P ratio of 90, the diameters of $MCN_{1.2}$, $MCN_{1.8}$, $MCN_{5.7}$, and $MCN_{7.3}$ were 151.5 ± 4.5 nm, 235.3 ± 4.5 nm, 211.6 ± 8.5 nm,

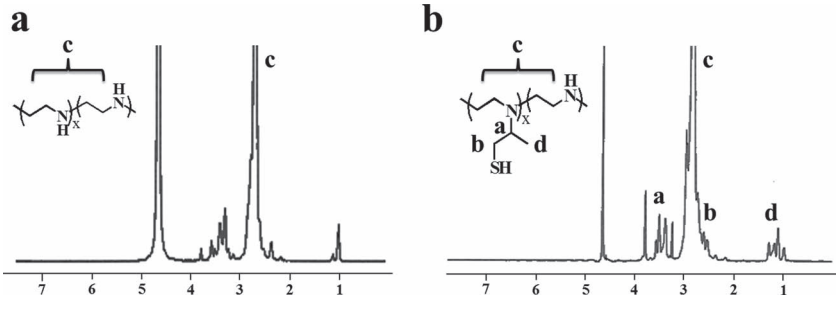

Figure 2. ^{1}H NMR spectra of a) LPEI and b) LPEI-$SH_{1.8}$.

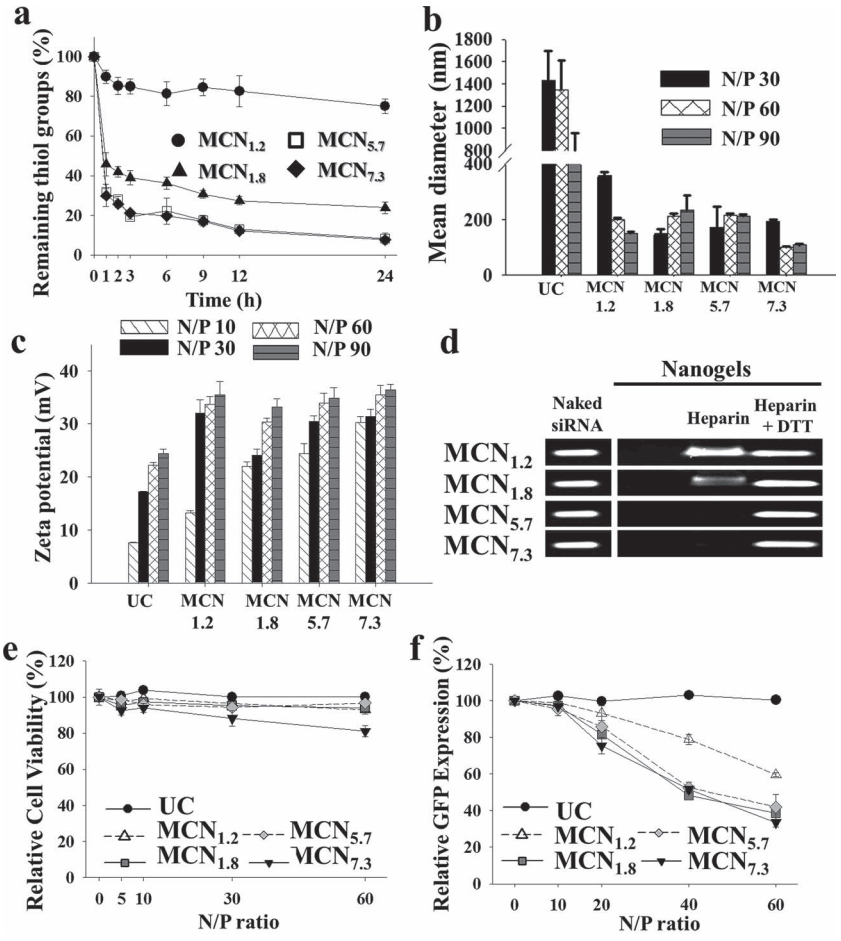

Figure 3. Effects of the crosslinking density on physicochemical properties of MCN_X (X = 1.2, 1.8, 5.7, and 7.3). a) Percentage of residual thiol groups in MCN_X at an N/P ratio of 60. b) Hydrodynamic mean diameter and c) zeta potential of MCN_X with different crosslinking densities determined from DLS analysis. d) Heparin/DTT decomplexation assay of MCN_X at an N/P ratio of 60 using agarose gel electrophoresis. e) Cytotoxicity and f) gene silencing efficiency of MCN_X in MDA-MB-435-GFP cells. The error bar indicates the standard deviation in triplicate experiments.

and 108.8 ± 3.1 nm, respectively. The diameter of nanogels was in the range of 300 to 100 nm regardless of the degree of thiolation in LPEI-SH_X at N/P ratios of 60 and 90. In particular, $MCN_{7.3}$ exhibited the smallest sizes, 101.5 nm and 108.8 nm at N/P ratios of 60 and 90, respectively, indicating the most effective condensation of siRNA within the nanogels presumably due to high crosslinking densities.

Although a significant percentage of secondary amine groups in MCN_X were substituted with thiol groups (e.g., about 12.6% for $MCN_{7.3}$), MCN_X exhibited a higher positive zeta potential than UC at all of N/P ratios (Figure 3c). At N/P ratios of 60 and 90, the zeta potential values of all of MCN_X were mostly in the range of +30–35 mV and only slightly increased with the increased N/P ratios possibly because the prepared nanogels had a very stable network structure that would not be affected by the addition of excess LPEI. On the contrary, UC exhibited relatively low zeta potential values (+22–24 mV), indicating the exposure of siRNA chains to the surface of polyelectrolyte complexes.

The structural stability of MCN_X was analyzed using a heparin-induced decomplexation assay. Without heparin treatment, no detectable amount of siRNA was dissociated from all of MCN_X as visualized using agarose gel electrophoresis (Figure 3d). However, the incorporated siRNAs within $MCN_{1.2}$ and $MCN_{1.8}$ were readily released in the presence of 100 mM heparin. Following the incubation with heparin, the nanogels were further treated with 200 mM 1,4-dithiolthreitol (DTT) to reduce the disulfide bonds of siRNA/LPEI inter- and intramolecular networks and dissociate the loaded siRNA from LPEI. Most of the loaded siRNAs were released in a monomeric form from all of the samples including $MCN_{5.7}$ and $MCN_{7.3}$. This result indicates that thiol-terminated siRNA was successfully complexed and chemically linked with thiol-grafted LPEI via disulfide bonds without significant loss during the nanogel formation.

The cytotoxicity of MCN_X was determined by measuring the cellular viability of human breast carcinoma cells expressing GFP (MDA-MB-435-GFP) treated with MCN_X at various N/P ratios. When the cells were treated with MCN_X up to an N/P ratio of 60 at an siRNA concentration of 144 nM, no significant cytotoxicity was observed for all of the MCN_X except $MCN_{7.3}$, as shown in Figure 3e. At an N/P ratio of 60, the viability of cells treated with $MCN_{7.3}$ slightly decreased to around 80%, which might be related to a higher level of cellular uptake in this condition. Figure 3f shows the GFP gene silencing activity of MCN_X on MDA-MB-435-GFP determined at various N/P ratios in the presence of 10% FBS. The siRNA concentration was fixed to 144 nM. It was revealed that the gene silencing efficiency increased with the increased N/P ratios, indicating that a highly compact, stable nanogel is more efficient for targeted gene silencing due to facile intracellular translocation.[29] $MCN_{1.2}$ exhibited relatively poor gene suppression because of insufficient structural stability. UC did not show any significant gene silencing activity under the experimental conditions used in our study because the molecular weight of LPEI was only 2.5 kDa, which seems to be too small to form a stable polyplex with siRNA, as the similar results were reported elsewhere.[30] In addition, a high molecular weight (25 kDa) of LPEI also exhibited negligible gene silencing activity for siRNA in our previous studies.[25,30] Interestingly, $MCN_{5.7}$ and $MCN_{7.3}$ showed similar gene silencing efficiency, indicating that about 5 thiol groups per LPEI backbone were sufficient to resist the dissociation and release of siRNA from the complex against excess anionic heparin molecules. Accordingly, $MCN_{5.7}$ was chosen for further characterization and biological evaluation. For comparison, UC and $LPEI_X$-siRNA nanogel (denoted CN_X) were used. Naked siRNA was used for CN_X, and thus the nanogel was formed only through the crosslinking between $LPEI_X$ chains.

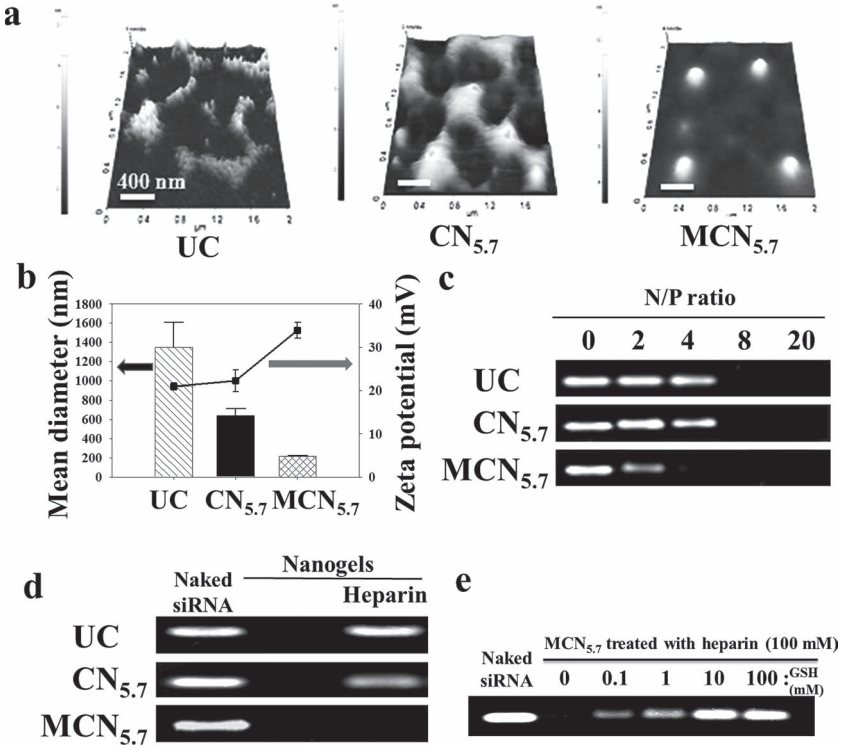

Figure 4. Physicochemical properties of UC, $CN_{5.7}$, and $MCN_{5.7}$. a) AFM images of each carrier at an N/P ratio of 60. Scale bar = 400 nm. b) Hydrodynamic mean diameters (bar graph, left panel) and zeta potentials (square, right panel) at an N/P ratio of 60 determined from DLS analysis. c) Electrophoretic migration of free siRNA from UC, $CN_{5.7}$, and $MCN_{5.7}$ prepared at different N/P ratios. d) Heparin-induced decomplexation assay using various carriers at an N/P ratio of 60. The concentration of heparin was 100 mM. e) Visualization of released siRNA from $MCN_{5.7}$ (N/P ratio = 60) in 100 mM heparin solution with increasing the GSH concentrations.

The morphology of UC, $CN_{5.7}$, and $MCN_{5.7}$ was examined using atomic force microscopy (AFM). $MCN_{5.7}$ was a well-dispersed spherical nanogel having an approximate diameter of about 200 nm, whereas $CN_{5.7}$ had irregular, larger structure, and UC was uneven and micrometer-sized aggregates (**Figure 4**a). The mean hydrodynamic diameters of UC, $CN_{5.7}$, and $MCN_{5.7}$ were 1427 ± 287 nm, 638 ± 72 nm, 215 ± 8 nm, respectively (Figure 4b). This result indicates that mutual crosslinking between siRNA and LPEI is critically important for the formation of a stable nanogel structure. Dehydration usually causes the shrinkage of a polymer hydrogel because of a low volume fraction of solid polymer. However, the size of dried $MCN_{5.7}$ from the AFM images was very similar to the hydrodynamic diameter presumably because the dehydration of nanogel did not affect the chain conformation presumably due to the highly compact structure of $MCN_{5.7}$. The zeta potential value of $MCN_{5.7}$ (34.9 ± 3.9 mV) was significantly higher than those of UC (21.4 ± 0.6 mV) and $CN_{5.7}$ (22.3 ± 2.5 mV). In $MCN_{5.7}$, thiol-terminated siRNA seems to be located within nanogels via intra- and intermolecular crosslinking. By contrast, a large number of naked siRNA might be only adsorbed on the surface of UC and $CN_{5.7}$ and thus easily diffuse out of complexes.

Electrophoretic migration of free siRNA from UC, $CN_{5.7}$, and $MCN_{5.7}$ prepared at different N/P ratios was examined using agarose gel electrophoresis (Figure 4c). At an N/P ratio of 4, no significant amount of siRNA was released from $MCN_{5.7}$, indicating that most of siRNA was complexed with LPEI-$SH_{5.7}$, while siRNA was readily released from UC and under the same condition. Heparin-induced decomplexation assay also showed that sj treated with 100 mM heparin exhibited no significant release of free siRNA, while UC and $CN_{5.7}$ showed an apparent band of free siRNA released from the complexes (Figure 4d). These results confirm that the crosslinks between siRNA and LPEI-$SH_{5.7}$ within $MCN_{5.7}$ can effectively prevent the dissociation of the complex by both of electric field and heparin via competitive ionic interaction.

The cytoplasm provides a reductive environment as the cytosolic concentration of glutathione (GSH) is in the range of 1 to 10 mM.[31,32] To confirm whether $MCN_{5.7}$ can be readily disintegrated in reductive condition, $MCN_{5.7}$ was incubated in 100 mM heparin solution containing GSH at various concentrations (0.1, 1, 10, and 100 mM). Free monomeric siRNA released from $MCN_{5.7}$ was quantified using agarose gel electrophoresis. The amount of siRNA released from $MCN_{5.7}$ increased with increasing the GSH concentrations, and most of the encapsulated siRNA was released at 10 mM GSH (Figure 4e). This result suggests that free monomeric siRNA can be dissociated from the nanogel through the cleavage of disulfide linkages following the cellular uptake, and monomeric siRNA can be regenerated and bind to RNA-induced silencing complex.[33,34] In addition, LPEI within the nanogels would also degrade to low molecular weight fragments, which are known to have lower toxicity, in the cytoplasm.

The cellular uptake of UC, $CN_{5.7}$, and $MCN_{5.7}$ was investigated using confocal microscopy with fluorescently labeled LPEIs: Cy5-labeled LPEI and Cy5-labeled LPEI-$SH_{5.7}$. UC did not show any significant cellular uptake, and a small number of $CN_{5.7}$ clusters were observed in the cytoplasm (**Figure 5**). By contrast, $MCN_{5.7}$ was internalized to a greater extent, shown as scattered red fluorescent dots in the cytoplasm (Figure 5). The smaller particle size and structural robustness of $MCN_{5.7}$ could contribute to the enhanced intracellular translocation of siRNA via endocytosis.[35,36]

The target-specific gene silencing activity by UC, $CN_{5.7}$, and $MCN_{5.7}$ was evaluated using MDA-MB-435-GFP cells in DMEM containing 10% FBS at various concentrations of siRNA (**Figure 6**a). $MCN_{5.7}$ exhibited a dose-dependent GFP silencing behavior and the far greater suppression of GFP expression, compared to UC and $CN_{5.7}$. At an siRNA concentration of 144 nM, the GFP expression level decreased to 45.8 ± 1.9% by $MCN_{5.7}$, whereas UC (96.59 ± 0.4%) and $CN_{5.7}$ (86.74 ± 1.2%) were not effective for gene silencing. The relative GFP expression of cells transfected with UC, $CN_{5.7}$, and

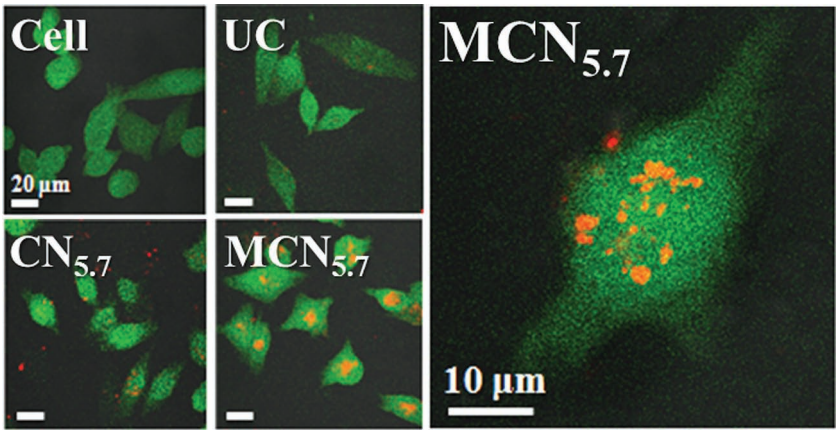

Figure 5. Confocal microscopy images of MDA-MB-435-GFP cells after the cellular uptake of Cy5-labeled carriers at an N/P ratio of 60 (left panel, scale bar = 20 μm). High magnification confocal image of the cell treated with $MCN_{5.7}$ (right panel, scale bar = 10 μm).

$MCN_{5.7}$ was also examined by fluorescence-activated cell sorting (FACS) analysis. $MCN_{5.7}$ showed a significant shift in GFP expressing cells population from 52.8% to 2.4%, while no significant changes were observed in the cells transfected with UC (47.3%) and $CN_{5.7}$ (36.0%), as shown in **Figure 6**b. We also examined gene silencing by therapeutically significant siRNA targeting vascular endothelial growth factor (VEGF) using UC, $CN_{5.7}$, and $MCN_{5.7}$ at an N/P ratio of 60. After the transfection with various complexes of VEGF siRNA into HeLa cells, the gene silencing effects were determined using enzyme-linked immunosorbent assay (ELISA). $MCN_{5.7}$-treated cells exhibited 23.5 ± 0.2% of VEGF expression, which was far lower than that of UC (98.1 ± 2.9%) and $CN_{5.7}$ (79.1 ± 4.7%) (Figure 6c), indicating that MCN can be exploited as an efficient delivery system for therapeutic siRNAs. To investigate whether the decreased protein expression of GFP and VEGF results from the degradation of intracellular mRNA, the levels of mRNA expression were determined using reverse transcriptase-polymerase chain reaction (RT-PCR) for the cells transfected with UC, and $MCN_{5.7}$. The relative band intensities of GFP mRNA were 99.4%, 91.5%, and 52.4% for UC, $CN_{5.7}$, and $MCN_{5.7}$, respectively, in MDA-MB-435-GFP cells (Figure 6d). The expression levels of VEGF mRNA in HeLa cells showed the similar results: UC (87.1%), $CN_{5.7}$ (89.2%), and $MCN_{5.7}$ (39.9%) (Figure 6e). Taken together, both of GFP and VEGF mRNAs were significantly suppressed to greater extents by $MCN_{5.7}$ compared to UC and $CN_{5.7}$, as

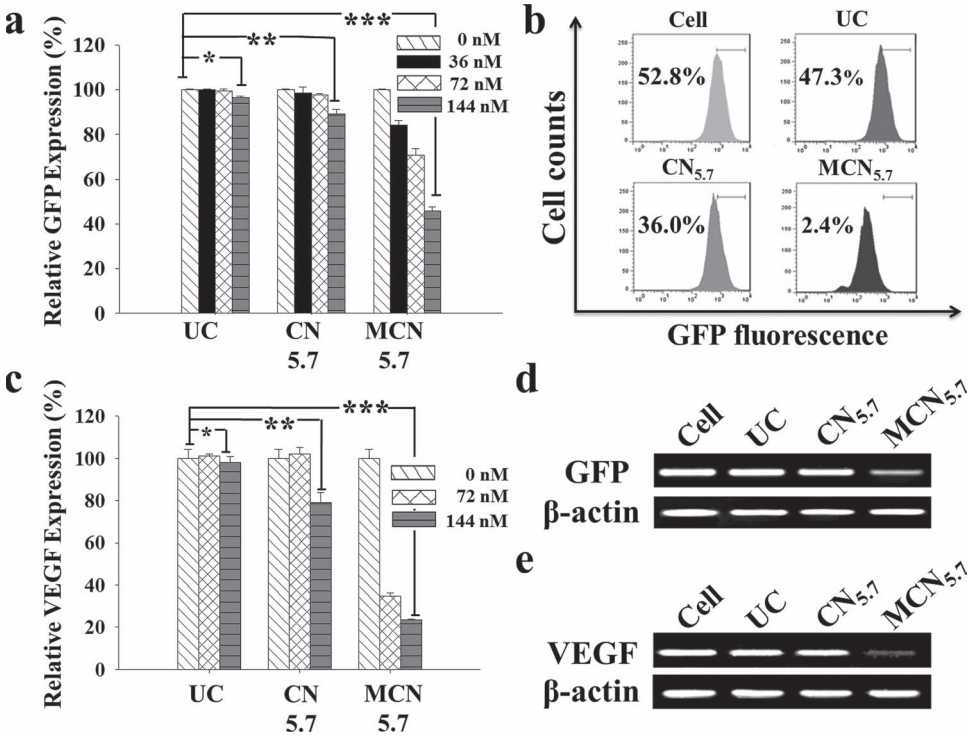

Figure 6. Comparison of the gene silencing activities of UC, $CN_{5.7}$, and $MCN_{5.7}$. a) Dose-dependent GFP inhibition efficiency after transfection with UC, $CN_{5.7}$, and $MCN_{5.7}$ at an N/P ratio of 60 for MDA-MB-435-GFP cells. *, **, and *** represent $P < 0.05$. b) FACS diagrams of the cells treated with different carriers. The percentage means the relative population of actively GFP expressing cells within a pre-determined arbitrary region, indicated with a bar. c) Target VEGF inhibition for HeLa cells after transfection with various carriers. * and ** represent $P < 0.05$. Semi-quantitative RT-PCR of intracellular GFP mRNA from MDA-MB-435-GFP cells (d) and VEGF mRNA from HeLa cells (e) after transfection. Human β-actin mRNA was used as a control.

consistent with the silencing levels of proteins. These results confirmed that the supression of GFP and VEGF expression in $MCN_{5.7}$-transfected cells was induced by the degradation of the corresponding mRNAs via RNAi processing.

3. Conclusions

In conclusion, this study demonstrated that a highly stable, compact nanogel comprising mutually crosslinked siRNA and LPEI exhibited enhanced cellular uptake and gene silencing efficiency. The electrostatic complexation and crosslinking between thiol-terminated siRNA and thiol-grafted LPEI, produced reductively dissociable nanogels containing inter- and intramolecular networks. The covalent linkages produced highly stable, compact nanogel structures that show very efficient intracellular translocation. Upon exposure to a reductive condition, the nanogel networks were readily dissociated, releasing biologically active, free monomeric siRNA that can effectively trigger RNAi-mediated gene silencing for the degradation of target mRNAs. The crosslinked LPEI also degraded into oligomeric LPEI (2.5 kDa), which is known to be less toxic than high molecular weight polyelectrolytes. Therefore, the mutually crosslinked siRNA/LPEI nanogel can be potentially utilized as an efficient intracellular delivery system for siRNA therapeutics.

4. Experimental Section

Materials: The primers and siRNAs targeting GFP and VEGF were purchased from Bioneer Co. (Daejeon, Republic of Korea). Each siRNA was modified with a thiol group at both 3′ ends. The siRNA and primer sequences were as follows: (GFP sense strand siRNA) 5′-AAC UUC AGG GUG AGC UUG CdTdT-3′; (GFP antisense strand siRNA) 5′-GCA AGC UGA CCC UGA AGU UdTdT-3′; (VEGF sense strand siRNA) 5′-GGA GUA CCC UGA UGA GAU CdTdT-3′; (VEGF antisense strand siRNA) 5′-GAU CUC AUC AGG GUA CUC CdTdT-3′; (forward GFP primer) 5′-TGG TGA GCA AGG GCG AGG AG-3′; (reverse GFP primer) 5′-GGG GGT GTT CTG CTG GTA GT-3′; (forward VEGF primer) 5′-AGG AGG GCA GAA TCA TCA CG-3′; (reverse VEGF primer) 5′-GAT CCG CAT AAT CTG CAT GGT-3′; (forward human p-actin primer) 5′-GTG GGG CGC CCC AGG CAC CAG GGC-3′; (reverse human p-actin primer) 5′-CTC CTT AAT GTC ACG CAC GAT TTC-3′. Heparin sodium salt (MW 12 kDa), DTT), dimethyl sulfoxide (DMSO), and diethylpyrocarbonate (DEPC) were purchased from Sigma (St. Louis, MO). 2-methylthiirane, 5, 5′-dithiobis-(-2-nitrobenzoic acid) (DTNB), and Cy5-maleimide were supplied from TCI (Tokyo, Japan), Pierce (Chester, UK), and GE Healthcare (Buckinghamshire, UK), respectively. LPEI (MW 2.5 kDa) was obtained from Polysciences, Inc. (Warrington, Pennsylvania). TRI Reagent, *Tag* DNA polymerase, and Omniscript RT-PCR kit were obtained from Ambion (Texas, USA), Takara (Tokyo, Japan), and Qiagen (Valencia, CA), respectively. Quantikine human VEGF immunoassay and EZ-cyTox cell viability assay kits were provided by R&D System (Minneapolis, MN) and Daeil Lab Service (Seoul, Republic of Korea), respectively. MDA-MB-435-GFP cell line was kindly donated by Samyang Co. (Seoul, Republic of Korea), and human epithelial carcinoma cells (HeLa) were purchased from Korean Cell Line Bank (Seoul, Republic of Korea). Dulbecco's modified Eagle medium (DMEM), fetal bovine serum (FBS), phosphate-buffered saline (PBS), and penicillin/streptomycin were obtained from Invitrogen (Carlsbad, CA).

Synthesis and Characterization of Thiol-Grafted LPEI (LPEI-SH_X): 10 μmol of LPEI were dissolved in 1 mL deionized water. After evaporating water under reduced pressure, the resulting product was dissolved in 1.5 mL methanol, and the solution was purged with argon for 5 min. To the solution was added various amounts of 10 vol% 2-methylthiirane (10, 30, 50, and 90 μmol) and reacted for 24 h at 50 °C. Each reaction mixture was evaporated under reduced pressure and kept under argon atmosphere. The final product was dissolved in PBS at pH 7.4, dialyzed and collected by lyophilization. The degree of thiol substitution in LPEI was determined by Ellman's method and ^1H NMR (400 MHz, D_2O): δ (ppm) = 3.53 (m, -CH-), 2.57 (m, $-CH_2-$), 2.58–2.92 (br, NCH_2CH_2N), 0.88-1.21 (br, CH_3). Four different LPEI-SH_X (the number of thiol groups grafted to each LPEI backbone, X = 1.2, 1.8, 5.7, and 7.3) were synthesized to control the crosslinking density in MCN_X. To prepare Cy5-labeled LPEI and LPEI-$SH_{5.7}$, LPEI-SH_1 and LPEI-SH_6 were synthesized by reacting 10 μmoles LPEI with 10 μmoles and 60 μmoles of 2-methylthiirane, respectively. 1 mg of each polymer dissolved in 1 mL deionized water was reacted with Cy5-maleimide (0.28 mg, 0.34 nmol) for 12 h at room temperature.

Preparation and Characterization of siRNA/LPEI Complexes: To prepare MCN_X, thiol-grafted $LPEI_X$ were dissolved in DEPC-treated PBS and complexed with 22 pmoles of thiol-terminated siRNA at both 3′-ends at different N/P ratios (from 2 to 90) for 20 min. The prepared complexes were further oxidized in 20 vol% DMSO under magnetic stirring at room temperature. After 24 h, DMSO was removed via dialysis and lyophilization, and the resulting complexes were dissolved in DEPC treated PBS. The remaining active thiol groups in each MCN_X were determined by Ellman's assay. UC was prepared by mixing LPEI and naked siRNA in DEPC-treated PBS, and CN was prepared using non-thiolated siRNA (naked siRNA) and LPEI-$SH_{5.7}$. The resulting complexes were visualized using a GelDoc-It TS imaging system (UVP, USA) following 1% agarose gel electrophoresis.

Stability and Cleavage Properties of siRNA/LPEI Complexes: To evaluate the structural stability of MCN_X, the oxidized MCN_X were incubated in 100 mM heparin with or without 200 mM DTT for 15 min. To determine the siRNA binding ability, UC, $CN_{5.7}$, and $MCN_{5.7}$ were prepared at N/P ratios of 2, 4, 8, and 20 with or without 100 mM heparin. In addition, $MCN_{5.7}$ at an N/P ratio of 60 were treated with 100 mM heparin and sequentially incubated with 0.1, 1, 10, and 100 mM of GSH for 15 min at room temperature. All reaction solutions were analyzed using 1% agarose gel electrophoresis.

Atomic Force Microscopy (AFM) and Dynamic Light Scattering (DLS): The diameter and morphology of $CN_{5.7}$ and $MCN_{5.7}$, formulated using LPEI-$SH_{5.7}$, and UC at an N/P ratio of 60 were observed by AFM (PSIA XE-100, Santa Clara, CA) in a non-contact mode. Each sample dissolved in DEPC-treated deionized water was spotted on a freshly cleaved mica surface (Pelco Mica sheets, Ted Pella Co.) and dried in air at room temperature. The diameter and zeta potential of the complexes at various N/P ratios were measured using DLS (Zetasizer Nano ZS, Malvern Instrument).

Gene Silencing: HeLa cells and MDA-MB-435-GFP cells were cultured in DMEM supplemented with 10% FBS, 100 units mL^{-1} penicillin, and 100 g mL^{-1} streptomycin in the humidified atmosphere with 5% CO_2 at 37 °C. For targeted GFP inhibition, MDA-MB-435-GFP cells were seeded in 12-well plates at a density of 1.5×10^5 cells/well for 24 h prior to transfection. The cells were transfected with UC, CN, and MCN at an N/P ratio of 60 with various siRNA concentrations in DMEM containing 10% FBS for 4 h. The cells were then washed with PBS and incubated in fresh culture medium for 24 h. To determine the extent of GFP expression, the transfected cells were lysed with 1 wt% Triton X-100 in PBS. Following the removal of cell debris by centrifugation, the intensity of GFP in the supernatants was determined using a spectrofluorophotometer (SLM-AMINCO 8100, SLM instrument, Rochester, NY) with excitation and emission wavelengths at 488 nm and 509 nm, respectively. The relative GFP expression was calculated on the basis of GFP level of non-treated MDA-MB-435-GFP cells. For FACS analysis, MDA-MB-435-GFP cells were also seeded on a 6-well plate at a density of 3×10^5 cells/well. The cells were transfected with the complexes at an N/P ratio of 60 for 4 h in 10% serum containing medium and replaced with fresh culture medium. The siRNA concentration was fixed at 144 nM. After 24 h incubation, the cells were detached using 0.05 wt-% trypsin and washed with PBS. After fixed with 3.7 wt% formaldehyde in PBS, the cells were analyzed using a flow

cytometer (FACScan, Becton Dickinson, USA). The FACS results were analyzed using CELLQUEST software (PharMingen, USA). For target VEGF silencing, HeLa cells were seeded in a 12-well plate at a density of 2×10^5 cells/well and further incubated for 24 h. Various siRNA/LPEI complexes were transfected into the cells in DMEM containing 10% FBS at an N/P ratio of 60 and various siRNA concentrations for 4 h. The medium was then replaced with fresh culture one, and the cells were further incubated for 24 h. The amounts of released VEGF in the culture medium were determined using a VEGF immunoassay kit.

Cell Viability Assay: MDA-MB-435-GFP cells were seeded in 96-well plates at a density of 1×10^4 cells/well and incubated for 24 h. The cells were treated with UC and MCN_X with 144 nM of siRNA at various N/P ratios in DMEM containing 10% FBS for 4 h. Then the cells were washed with PBS and incubated with fresh culture medium. After further incubation for 48 h, the amount of viable cells was evaluated staining with the tetrazolium salt containing solution (EZ-cyTox).

Cellular Uptake Efficiency: MDA-MB-435-GFP cells were seeded in a 4-well chamber at a density of 2×10^5 cells/well and incubated for 24 h. By using Cy5-conjugated LPEI or LPEI-$SH_{5.7}$, dye-labeled UC, CN_5, and MCN_5 were prepared at an N/P ratio of 60.

These complexes were transfected into the cells in DMEM containing 10% FBS. The siRNA concentration was fixed at 144 nM. After 2 h incubation, the cells were washed three times with PBS and fixed with 3.7 wt% formaldehyde solution in PBS for 20 min at room temperature. The cellular uptake of Cy5-labeled complexes was visualized using confocal laser scanning microscopy (LSM 510, Carl Zeiss, USA).

Reverse Transcriptase Polymerase Chain Reaction (RT-PCR): MDA-MB-435-GFP cells or HeLa cells were proliferated on a 6-well plate at a density of 3×10^5 cells/well for 24 h. The cells were transfected with UC, $CN_{5.7}$, and $MCN_{5.7}$ containing 144 nM of siRNA for MDA-MB-435-GFP cells and 75 nM of siRNA for HeLa cells at an N/P ratio of 60. After incubation for 4 h in DMEM containing 10% FBS for 4 h, the cells were replaced with fresh culture medium and further incubated for 24 h. Two micrograms of total RNA, extracted from each transfected cell by using TRI Reagent were reversely transcribed to cDNA at 37 °C for 2 h and 93 °C for 5 min using an Omniscript RT-PCR kit. Each cDNA was subsequently amplified using *Tag* polymerase and their specific primer sets. The PCR conditions of GFP and human β-actin mRNAs were as follows: denaturation, 1 cycle at 94 °C for 5 min; amplification, 21 cycles at 94 °C for 30 s, at 60 °C for 30 s, and at 72 °C for 40 s; final extension, 1 cycle at 72 °C for 10 min. For the amplification of VEGF mRNA, 26 cycles were performed. The relative amount of PCR products was compared using 1% agarose gel electrophoresis with EtBr staining.

Statistical Analysis: All of data were represented with a mean value ± standard deviation from independent measurements. Statistical analysis was performed with a Student's t-test. Statistical significance was assigned for *P*-values <0.05 (95% confidence level).

Acknowledgements

All authors deeply thank the late Professor Tae Gwan Park for his invaluable contribution, educational efforts, and inspiration. This study was supported by a grant of the Korea Healthcare Technology R&D Project (A040041 and A111552), Ministry of Health and Welfare, Republic of Korea. C.A.H. and J.S.K. contributed equally to this work.

Received: March 2, 2012
Revised: June 3, 2012
Published online: August 24, 2012

[1] Y. K. Oh, T. G. Park, *Adv. Drug Delivery Rev.* **2009**, *61*, 850.
[2] A. P. McCaffrey, L. Meuse, T. T. Pham, D. S. Conklin, G. J. Hannon, M. A. Kay, *Nature* **2002**, *418*, 38.
[3] A. de Fougerolles, H. P. Vornlocher, J. Maraganore, J. Lieberman, *Nat. Rev. Drug Discovery* **2007**, *6*, 443.
[4] K. A. Whitehead, R. Langer, D. G. Anderson, *Nat. Rev. Drug Discovery* **2009**, *8*, 129.
[5] J. H. Jeong, H. Mok, Y. K. Oh, T. G. Park, *Bioconjugate Chem.* **2009**, *20*, 5.
[6] J. H. Kuo, Y. L. Lo, M. D. Shau, J. Y. Cherng, *J. Controlled Release* **2002**, *81*, 321.
[7] M. Ikonen, L. Murtomaki, K. Kontturi, *Colloids Surf. B: Biointerfaces* **2008**, *66*, 77.
[8] A. K. Varkouhi, G. Mountrichas, R. M. Schiffelers, T. Lammers, G. Storm, S. Pispas, W. E. Hennink, *Eur. J. Pharm. Sci.* **2012**, *45*, 459.
[9] D. J. Gary, N. Puri, Y. Y. Won, *J. Controlled Release* **2007**, *121*, 64.
[10] H. Lee, H. Mok, S. H. Lee, Y. Oh, T. G. Park, *J. Controlled Release* **2007**, *119*, 245.
[11] S. Boeckle, K. von Gersdorff, S. van der Piepen, C. Culmsee, E. Wagner, M. Ogris, *Gene Med.* **2004**, *6*, 1102.
[12] L. De Laporte, J. Cruz Rea, L. D. Shea, *Biomaterials* **2006**, *27*, 947.
[13] D. Putnam, C. A. Gentry, D. W. Pack, R. Langer, *Proc. Natl. Acad. Sci. USA* **2001**, *98*, 1200.
[14] T. G. Park, J. H. Jeong, S. W. Kim, *Adv. Drug Delivery Rev.* **2006**, *58*, 467.
[15] Z. Hassani, G. F. Lemkine, P. Erbacher, K. Palmier, G. Alfama, C. Giovannangeli, J. P. Behr, B. A. Demeneix, *Gene Med.* **2005**, *7*, 198.
[16] V. Sokolova, M. Epple, *Angew. Chem. Int. Ed.* **2008**, *47*, 1382.
[17] A. L. Bolcato-Bellemin, M. E. Bonnet, G. Creusat, P. Erbacher, J. P. Behr, *Proc. Natl. Acad. Sci. USA* **2007**, *104*, 16050.
[18] S. H. Lee, H. Mok, S. Jo, C. A. Hong, T. G. Park, *Biomaterials* **2011**, *32*, 2359.
[19] C. A. Hong, S. H. Lee, J. S. Kim, J. W. Park, K. H. Bae, H. Mok, T. G. Park, H. Lee, *J. Am. Chem. Soc.* **2011**, *133*, 13914.
[20] Q. Peng, Z. L. Zhong, R. X. Zhuo, *Bioconjugate Chem.* **2008**, *19*, 499.
[21] Y. L. Lin, G. Jiang, L. K. Birrell, M. E. El-Sayed, *Biomaterials* **2010**, *31*, 7150.
[22] V. Knorr, M. Ogis, E. Wagner, *Pharm. Res.* **2008**, *25*, 2937.
[23] D. Jere, H. L. Jiang, R. Arote, Y. K. Kim, M. H. Cho, T. Akaike, C. S. Cho, *Expert. Opin. Drug Delivery* **2009**, *6*, 827.
[24] M. Breunig, U. Lungwitz, R. Liebl, A. Goepferich, *Proc. Natl. Acad. Sci. USA* **2007**, *104*, 14454.
[25] H. Mok, S. H. Lee, J. W. Park, T. G. Park, *Nat. Mater.* **2010**, *9*, 212.
[26] M. Nakanishi, R. Patil, Y. Ren, R. Shyam, P. Wong, H. Q. Mao, *Pharm. Res.* **2011**, *28*, 1723.
[27] A. Tamura, M. Oishi, Y. Nagasaki, *Biomacromolecules* **2009**, *10*, 1818.
[28] H. J. Chung, C. A. Hong, S. H. Lee, S. Jo, T. G. Park, *Bioconjugate Chem.* **2011**, *22*, 299.
[29] J. H. Ryu, R. T. Chacko, S. Jiwpanich, S. Bickerton, R. P. Babu, S. Thayumanavan, *J. Am. Chem. Soc.* **2010**, *132*, 17227.
[30] S. H. Lee, H. Mok, Y. Lee, T. G. Park, *J. Controlled Release* **2011**, *752*, 152.
[31] T. Okamoto, T. Akaike, T. Sawa, Y. Miyamoto, A. Van der Vliet, H. Maeda, *Biol. Chem.* **2001**, *276*, 29596.
[32] K. Miyata, Y. Kakizawa, N. Nishiyama, A. Harada, Y. Yamasaki, H. Koyama, K. Kataoka, *J. Am. Chem. Soc.* **2004**, *126*, 2355.
[33] S. H. Kim, J. H. Jeong, S. H. Lee, S. W. Kim, T. G. Park, *J. Controlled Release* **2006**, *116*, 123.
[34] M. Z. Zhang, A. Ishii, N. Nishiyama, S. Matsumoto, T. Ishii, Y. Yamasaki, K. Kataoka, *Adv. Mater.* **2009**, *21*, 3520.
[35] A. C. Grayson, A. M. Doody, D. Putnam, *Pharm. Res.* **2006**, *23*, 1868.
[36] W. H. Kong, K. H. Bae, C. A. Hong, Y. Lee, S. K. Hahn, T. G. Park, *Bioconjugate Chem.* **2011**, *22*, 1962.